A METHODOLOGY BASED ON OPERATIONAL MODAL ANALYSIS TO ESTIMATE MODAL PARAMETERS AND CUTTING FORCES IN REAL TIME.

Tatiana Meola, tatiana.meola@gmail.com
Vinícius Abrão da Silva Marques, vinicius.abrao@hotmail.com
Universidade Federal de Uberlândia, Av. João Naves de Ávila, 2121 - Campus Santa Mônica, Bloco 1M, Uberlândia - Mg, CEP 38400-902

Marcus Antonio Viana Duarte, mvduarte@mecanica.ufu.br
Universidade Federal de Uberlândia, Av. João Naves de Ávila, 2121 - Campus Santa Mônica, Bloco 1M, Uberlândia - Mg, CEP 38400-902

Abstract. *Tool condition monitoring by vibration analysis has been used due to the good agreement among measured vibration and tool wear, surface finish and cutting forces, for example. The main problem of this approach is that the vibration levels are strongly dependent of the dynamic characteristics of process which is also dependent of machine conditions and transmission path. So, prefixed vibration symptom limits can be changed due to machines setup such as: preload of the fixing screws of the tool, position of the tool port, vibration symptoms of the drive devices, among others. The aim of this work is present a methodology to contour it. The approach is based on Operational Modal Analysis and Minimum Realization System to estimate the dynamics cutting efforts by real time monitoring of magazine tools vibrations. The methodology was validated numerically using a finite elements model of a magazine tool submitted to triaxial cutting forces. To make it two sets of three sensors response located on optimized places was used.*

Keywords*: Operational Modal Analysis; Modal Parameters; Cutting Forces*

1. INTRODUCTION

Tool condition monitoring by vibration analysis has been used due to the good agreement among measured vibration and tool wear, surface finish and cutting forces. The main problem of this application is that the vibration levels dependent of the dynamic characteristics of mechanical system and its transmission path. Consequently, the vibration symptoms limits besides being valid for a specific machine can also change depending on the setup of the machine such as: preload of the fixing screws of the tool, position of the tool port, vibration symptoms of the drive devices, among others

To minimize this problem Operational Modal Analysis (OMA) technique can be used. This technique is applied to get modal dynamic model of systems with unknown natural excitation forces using output only (Mohanty et al, 2003).

Classical estimation of modal parameters is based on Impulse Response Function FRI or Frequency Response Function FRF obtained in controllable laboratory conditions. However, in many cases real operational conditions may differ from those applied during the modal test. This problem is even greater when only the response data are measurable while the loading conditions are unknown. (Hermans et al, 1999).

With this, operational modal analysis is an analyzing technique for structures subjected to an excitation generated by its own process (Mohanty et al, 2003), as the case of cutting processes.

According to Zhang et al (2005), OMA, also known as NExT (Natural Excitation Technique), is a technique that suggests the use of correlation function of structure random response subjected to a natural excitation. NExT has shown that the correlation COR can be expressed as a summation of decaying sinusoids. Each decaying sinusoid represents one damped natural frequency, damping ratio and mode shape coefficient of the complete multi degree-of-freedom studied model. COR can therefore be employed as impulse response function (IRF) to estimate modal parameters. Hence, major multi-input/multi-output ((MIMO) modal identification procedures can be adopted for OMA. In this work a MIMO technique based on Eigensystem Realization Algorithm ERA was used.

1.2. The minimum realization theory

To construct a model, a fundamental question immediately arises as to whether or not all the system states of interest can be excited (controlled) and/or observed. (Juang, 1994). From a space of states system it's possible to derive theories which investigate whether all spaces can be controlled and / or observed. (Alves, 2005). Given a time invariant system:

$$\{\dot{u}(t)\} = [A_c]\{u(t)\} + [B_c]\{w(t)\} \quad (1)$$

$$\{y(t)\} = [C_c]\{u(t)\} + [D_c]\{w(t)\} \quad (2)$$

which representation at discrete time is given by:

$$u(k+1) = A'u(k) + B'w(k) \tag{3}$$

$$y(k) = C'u(k) + D\,w(k) \tag{4}$$

where:
u is state vector (2N × 1);
w is input vector or control (q × 1), considered a random signal;
y is output vector, measured responses (p × 1);
A_c and A' are state matrices that describe the system dynamics at continuous and discrete domains, respectively (2N X 2N);
B_c and B 'are the input matrices in the continuous and discrete domains, respectively (2N X q);
C_c and C' are sensor matrices (p X 2N), the system output to the state vector u, in the continuous and discrete domains, respectively.
D_c and D are direct transmission matrices (p X q), continuous and discrete domains, respectively.

Once that mass matrix is positive definite, $\{\ddot{x}\}$ can be obtained by manipulation of Eq. 5 resulting in Eq. 6. In this equation, $\{f(t)\}$ is given by product $\left[B_f\right]\{w(t)\}$, where and [Bf] is the input influence matrix.

$$[M]\{\ddot{x}(t)\} + [C]\{\dot{x}(t)\} + [K]\{x(t)\} = \{f(t)\} \tag{5}$$

$$\{\ddot{x}(t)\} = -[M]^{-1}[C]\{\dot{x}(t)\} - [M]^{-1}[K]\{x(t)\} + [M]^{-1}\{f(t)\} \tag{6}$$

To include the acceleration response into the output vector, one relation shown by Nunes (2006), can be used:

$$\{y(t)\} = [C_a]\{\ddot{x}(t)\} \tag{7}$$

where [Ca] describe the relation between vector $\{\ddot{x}(t)\}$and output vector $\{y(t)\}$.

Substituting Eq. 6 in 7, one has:

$$\{y(t)\} = [C_a][M]^{-1}\left[[B_f]\{w(t)\} - [C]\{\dot{x}(t)\} - [K]\{x(t)\}\right] \tag{8}$$

In compact form:

$$\{y(t)\} = [C_c]\{u(t)\} + [D_c]\{w(t)\} \tag{9}$$

where $[C_c] = \left[-[C_a][M]^{-1}[K] \quad -[C_a][M]^{-1}[C]\right]$ e $[D_c] = -[C_a][M]^{-1}[B_f]$.

The system response for any input can be determined by Eq. 3 and 4 (Juang, 1994).
At time tf, the solution of Eq. 1 is given by:

$$u(t_f) = e^{A_c(t-t_0)}u(t_0) + \int_{t_0}^{t_f} e^{A_c(t_f-\tau)}\,B_c w(\tau)d\tau \tag{10}$$

for $t \geq t0$. The solution for discrete representation, Eq. 3, at time $tf = k\Delta t$, where Δt is the sampling time, can be represented by:

$$u(k) = A'^{(k)}\, u(0) + \sum_{i=1}^{k} A'^{(i-1)}\, B'\, w(k-i) \tag{11}$$

or in matricial form by:

$$u(p) = A^{k} u(0) + \begin{bmatrix} B' & A'B' & A'^{2}B' & \cdots & A'^{(k-1)}B' \end{bmatrix} \begin{bmatrix} w(k-1) \\ w(k-2) \\ w(k-3) \\ \\ w(0) \end{bmatrix} \tag{12}$$

where u(0) = u(t0) is the initial state at t = t0.

Substituting w_i (0) = 1 (i = 1, 2, ..., r) and w_i (k) = 0 (k = 1, 2, ...) into Eq. 3 e 4 for each input element, the results can be constructed in a impulse response matrix Y with dimensions $(p \times 2N)$.

$$Y_0 = D, \quad Y_1 = C'B', \quad Y_2 = C'A'B', \quad \cdots, \quad Y_k = C'A'^{k-1}B' \tag{13}$$

Given the response y(k), vector u (Eq. 2) can be determined, assuming initial condition D.w(k) zero and using a minimum realization algorithm to estimate C'.

After determination of u(k+1) and u(k), w(k) can be estimated. The matrix A' and B' were obtained previously by ERA.

2. OBJECTIVE

The aim of this work is the study of the use of Next and ERA to identify triaxial forces applied to a turning magazine tool model.

3. METHODOLOGY

A turning magazine tool model was developed by finite elements showed in Fig. 1 (structural model) and 2 (mesh).

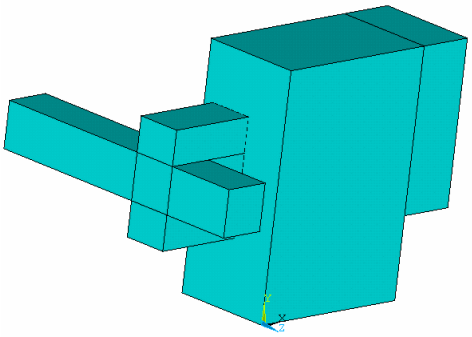

Figure 1. Model volumes

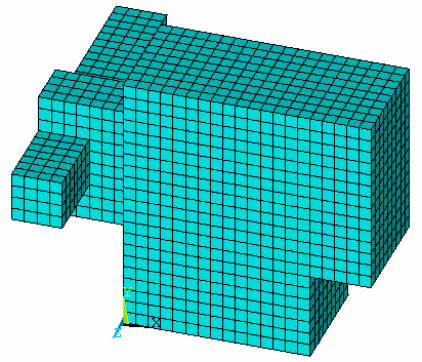

Figure 2. Model Elements

To simulate the cutting excitation, three random forces were applied in node 4602 (Fig. 3), the supposed edge tool, at directions X, Y and Z. To simulate the dynamic behavior of the model was used a modal model of 10 degrees of freedom obtained by finite elements and Parseval's theorem to get the time responses of the chosen nodes (see Fig. 3). The criterion used to choice the nodes was based on 10 modal shapes of the model. The damping factors for all modes were of 0.06 (6%) and the resultant natural frequencies were: 1814, 2045, 2745, 3309, 3605, 6141, 6774, 8712, 8974 and 9567 Hz.

A sensibility analysis was carried out to determine which of the 12 nodes are more interesting to place the vibration sensors. The selection criterion was based on the results of better random force identification. So, the forces spectrum behavior were analyzed and compared. Due to the fact that each node have three displacement responses and

three velocities responses (directions X, Y and Z), using the three one displacement as reference, the tests were carried out with 6 sensors.

The velocities and displacement responses were simulated with a sampling rate of 25000 Hz and total acquisition time of 20s. The correlation functions were estimated by fft (512 samples and Hanning window) which results in FRIs with dimension of 128×1. The resultant frequency resolution was df = 49 Hz.

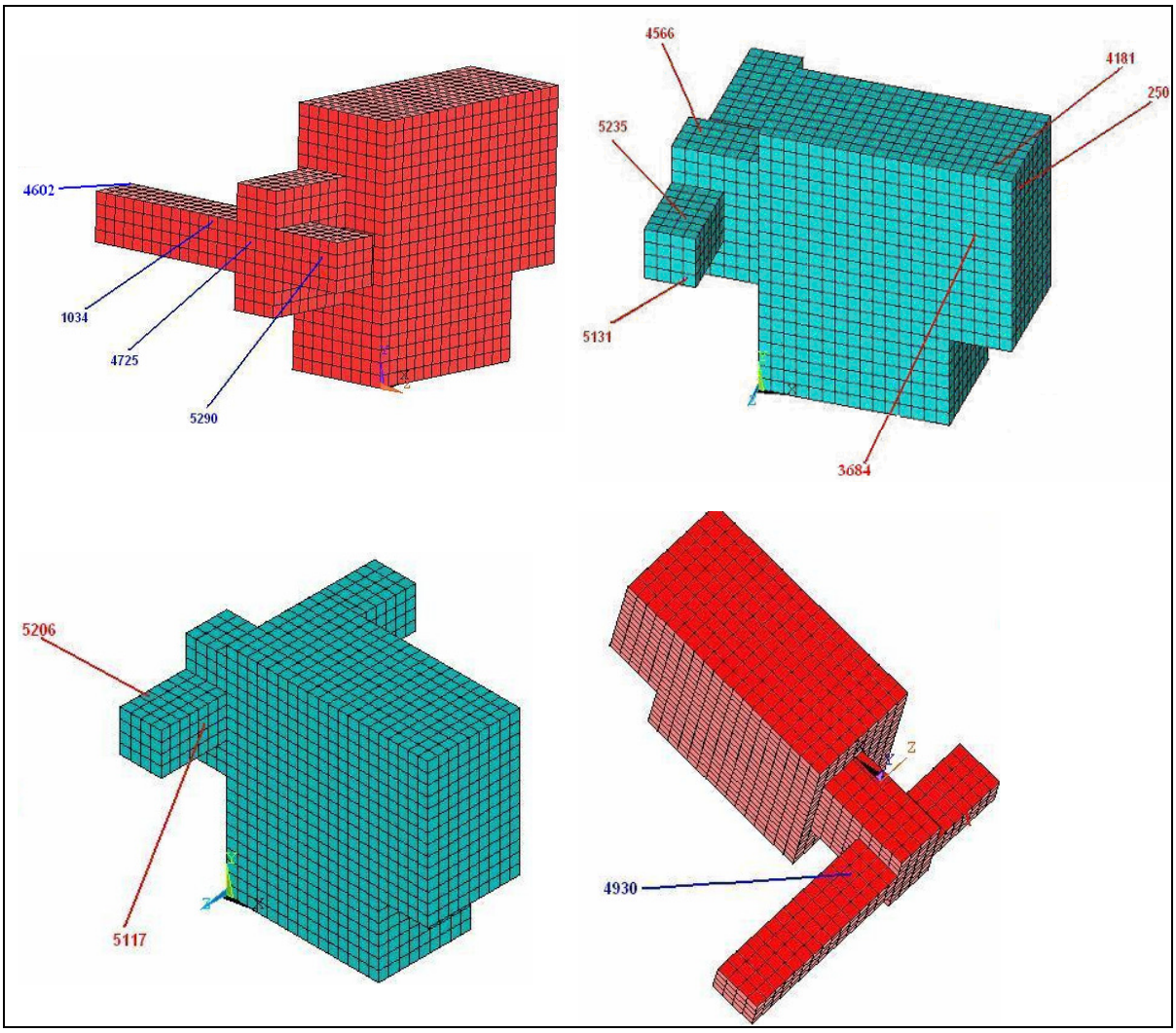

Figure 3. Finite Element Nodes position.

According to Nunes (2006), the number of row blocks i of Hankel matrix is a variable previously defined to be higher enough, with li ≥ n, where n (2N) is the system order to be identified and l is the sensor number. When n is unknown at priori it is assumed that i = 2.nl. The number of columns is given by j = (npontos) - 2i + 1, where "npontos" is the length of the response vectors.

Thus, as example, according to FRI shown in Fig. 4, it is possible to determine "npontos", rows (r) and columns of the Hankel(s) matrix.

The “npontos” of 100 was chosen due to the fact that the IRF amplitudes vanish upper it (See Fig. 4). Consequently, for 6 responses, the calculated values to r and s are:

r = 2*2*10/6 = 6.667
s = 100 – (2*r) + 1 = 87.667

In resume, were chosen r = 14 (multiple of 7) and s = 88.

The premise used in this work is that experimental apparatus is constituted by two triaxial accelerometers. By integration 12 responses can be used (6 velocities and 6 displacements), which results in r=12 (multiple of 3) and s =94.

As input, two harmonic signals of 60 Hz and 500 Hz and a random signal were used to simulate an usual rotative machine loads condition. The effect of extraneous noise was not modeled because vibration tests based in operational

conditions, only structures responses are measured and the entry is assumed random and it's not measured, therefore it's impossible to distinguish the system entry of the noise terms. If the entry feature is a typical of a white noise, this can be modeled implicitly by the noise terms, resulting in a purely random system (Nunes, 2006).

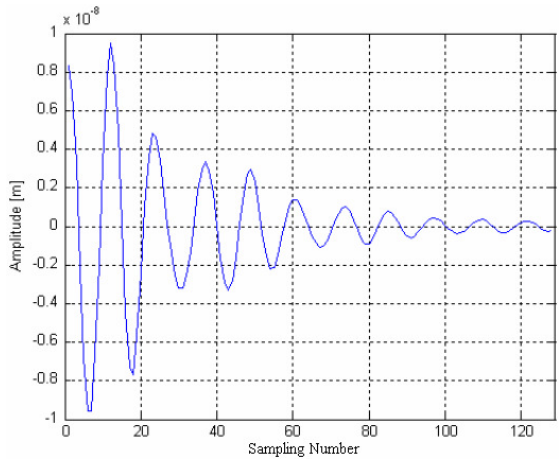

Figure 4. Impulse Response Function of response at Y on node 250.

Established the meta-model through Next approach, the next step consist in estimate the input forces given the simulated responses. The frequency range is upper limited by the highest meta-model natural frequency. According to Duarte (1994), accurate frequency response is obtained to excitation frequencies below than 0.5 times the higher natural frequency of the modal model. To make it, in this work the simulated responses was filtered using a sixth order type I Chebyshev (0.5 dB ripple) low pass filter.

4. RESULTS

4.1. Sensibility Analysis.

Of the sensibility analysis the nodes that presented goods results were: 250; 3684; and 4725.

In Table 1 are shown the natural frequencies f, damping rates ζ, MAC values (Modal Amplitude Coherence) and MSV values (Modal Singular Value) estimated to sensors placed at node 250.

Maximum degrees of freedom number must be three, to invert the matrix C 'and identify the excitation w of Eq. 1, due to a node has six responses. As the highest system natural frequency is 3573 Hz, the cut off frequency used to filter the output response is 1700 Hz. Thus, Fig. 5 shows the power spectrum of estimated forces at directions X, Y and Z, and the power spectrum of simulated force. All spectrums were calculated with 4096 samples, 50% of overlap and to esthetical effects are shown until 6000 Hz.

Table 1. Estimated natural frequency *f* and damping rates ζ for the system in the node 250

Estimated ζ (%)	Estimated *f* (Hz)	Simulated ζ (%)	Simulated *f* (Hz)	MAC	MSV
6.4	2047	6.0	2045	0.99	37.2
5.3	2765	6.0	2745	0.35	8.6
8.5	3573	6.0	3605	0.94	4.3

The choice of this node reside on similar shape between estimated and simulated forces power spectrums. The observed differences between magnitudes occur because the random excitation force is unknown at Next procedure. Therefore, the forces are often estimated with an unknown a priori calibration factor. The differences of 2 Hz, 20 Hz and 32 Hz between fitted frequencies and simulated natural frequencies are in accordance to frequency resolution of the analysis (± 49 Hz). Damping rates have differences of 0.4 %, 0.7 % e 2.5 %.

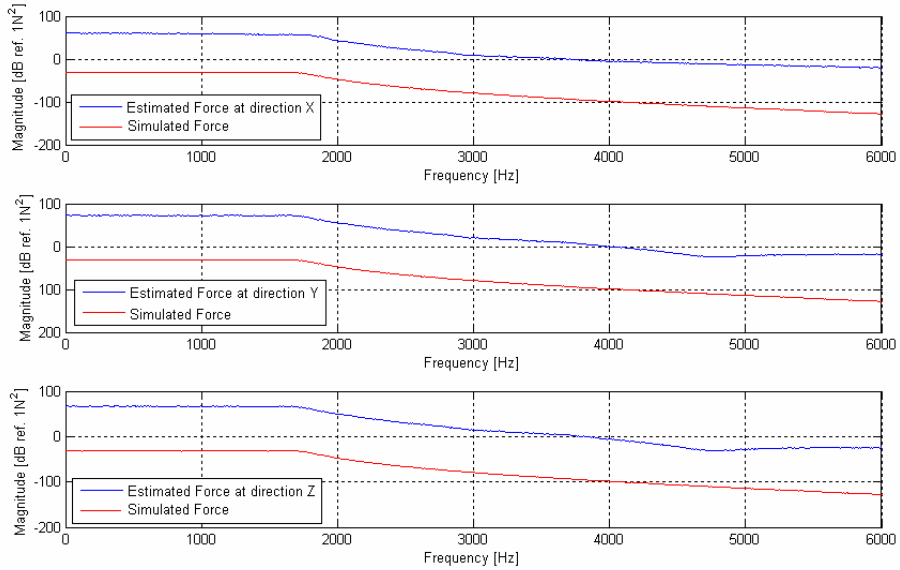

Figure 5. Power spectrum of estimated forces at directions X, Y and Z, and the power spectrum of simulated force for node 250.

In Table 2 are shown the natural frequencies f, damping rates ζ, MAC values (Modal Amplitude Coherence) and MSV values (Modal Singular Value) estimated to sensors placed at node 3684.

Table 2. Estimated natural frequency *f* and damping rates ζ for the system in the node 3684

Estimated ζ (%)	Estimated *f* (Hz)	Simulated ζ (%)	Simulated *f* (Hz)	MAC	MSV
6.3	2046	6.0	2045	0.98	35.3
9.8	2746	6.0	2745	0.94	8.3
6.5	3508	6.0	3605	0.75	6.4

Power spectrum of estimated forces at directions X, Y and Z, and the power spectrum of simulated force are presented in Fig. 6.

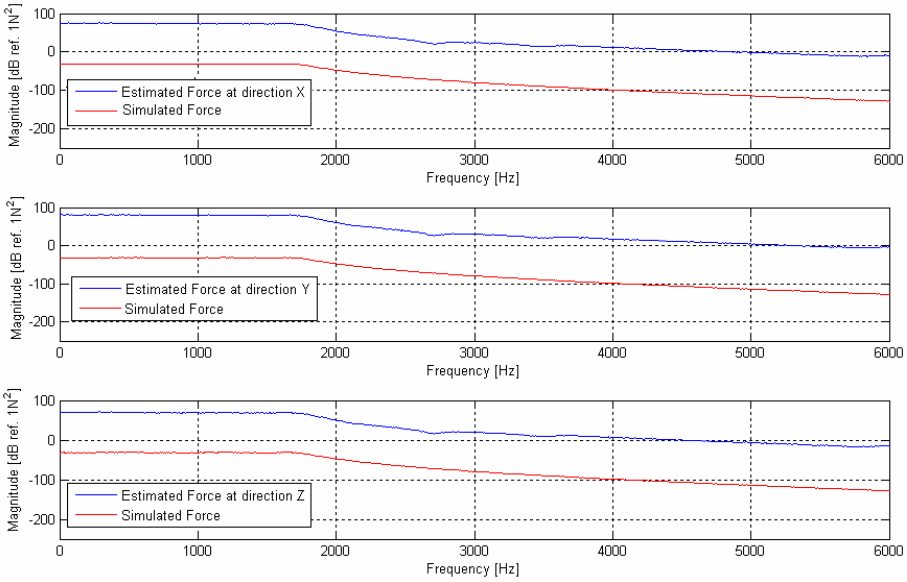

Figure 6. Power spectrum of estimated forces at directions X, Y and Z, and the power spectrum of simulated force for node 3684.

This node was also chosen because presents similar shape between estimated and simulated forces power spectrums. The differences of 1 Hz between fitted frequencies and simulated natural frequencies for the two first identified modes are in accordance to frequency resolution of the analysis. For estimated frequency of 3508 Hz the difference is about 97 Hz. This variation didn't affect the force estimation (see Fig. 6), mainly due to the fact of responses were filtered with a low pass cut frequency of 1700 Hz.

In Table 3 are shown the natural frequencies f, damping rates ζ, MAC values (Modal Amplitude Coherence) and MSV values (Modal Singular Value) estimated to sensors placed at node 4725. The correspondent power spectrum of estimated forces at directions X, Y and Z, and the power spectrum of simulated force are presented in Fig. 7.

Table 3. Estimated natural frequency *f* and damping rates ζ for the system in the node 4725

Estimated ζ (%)	Estimated *f* (Hz)	Simulated ζ (%)	Simulated *f* (Hz)	MAC	MSV
6.9	1811	6.0	1814	0.42	20.5
6.3	2046	6.0	2045	0.72	23.2
6.7	3543	6.0	3605	0.56	6.4

In Tab.3, the differences between fitted and simulated damping rates are 0.9%, 0.7% e 0.3% for frequencies of 1811, 2046 and 3543 Hz, respectively. For estimated frequency of 3543 Hz the frequency difference is higher than 49 Hz.

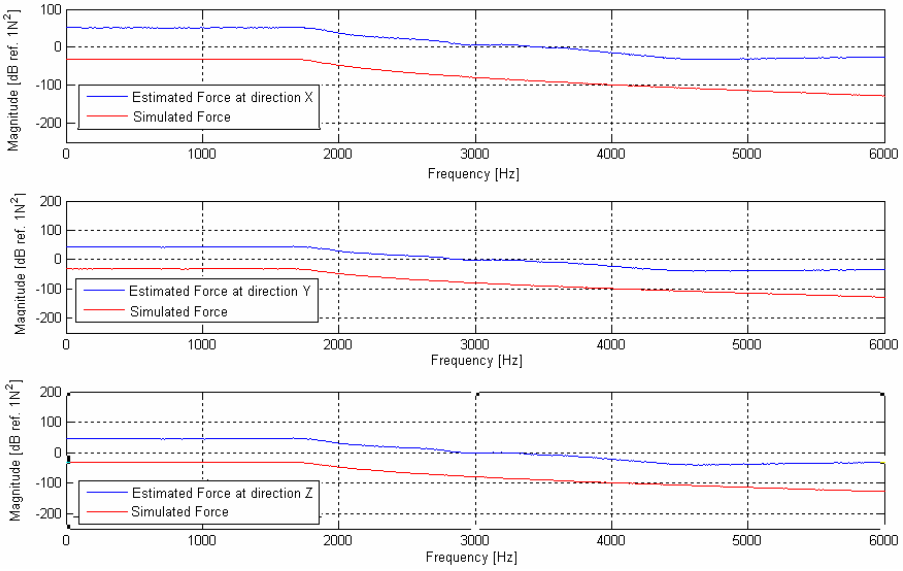

Figure 7. Power spectrum of estimated forces at directions X, Y and Z, and the power spectrum of simulated force for node 4725.

4.2. Two nodes combination.

The combination that presents the best forces identification was node 3684 with node 4725, using the node 3684 as reference.

In Table 4 are shown the natural frequencies f, damping rates ζ, MAC values (Modal Amplitude Coherence) and MSV values (Modal Singular Value) estimated to sensors placed at nodes 3684 and 4725.

In Table 4 estimated damping rates for fitting model are close to 6% and the highest difference in relation to the simulated model values is 1.8%.

Power spectrum of estimated forces at directions X, Y and Z, and the power spectrum of simulated force are presented in Fig. 8. One can observe in Fig. 8 that there is a good agreement between curves of the estimated and simulated power spectrums.

Table 4. Estimated natural frequency *f* and damping rates ζ for 3684 and 4725 nodes combination.

Estimated ζ (%)	Estimated *f* (Hz)	Simulated ζ (%)	Simulated *f* (Hz)	MAC	MSV
5.8	1819	6.0	1814	1.00	9.2
6.1	2048	6.0	2045	1.00	28.8
5.9	2764	6.0	2745	0.96	4.8
5.7	3607	6.0	3605	0.83	5.4
5.9	6141	6.0	6141	0.28	1.3
7.2	8994	6.0	8974	0.87	0.4

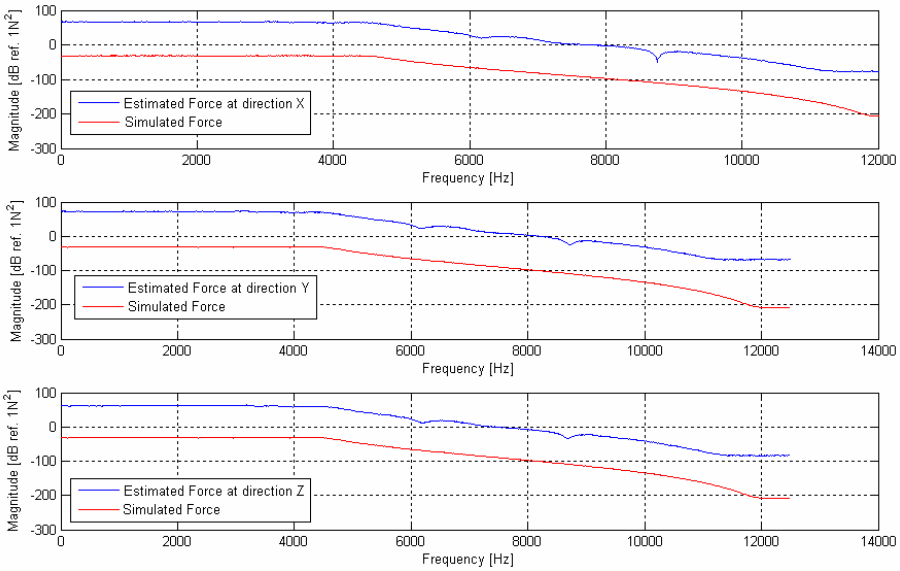

Figure 8. Power spectrum of estimated forces at directions X, Y and Z, and the power spectrum of simulated force for combination of 3684 and 4725 nodes.

In Table 5 are shown the natural frequencies *f*, damping rates ζ, MAC values (Modal Amplitude Coherence) and MSV values (Modal Singular Value) estimated for force simulation at harmonic components and random noise presence.

Table 5. Estimated natural frequency *f* and damping rates ζ for simulation of force in presence of harmonic components and random noise.

Estimated ζ (%)	Estimated *f* (Hz)	Simulated ζ (%)	Simulated *f* (Hz)	MAC	MSV
5.7	1819	6.0	1814	1.00	9.3
6.1	2049	6.0	2045	1.00	29.0
5.9	2761	6.0	2745	0.96	4.8
5.7	3608	6.0	3605	0.83	5.4
5.9	6122	6.0	6141	0.21	1.3
16.0	8496	6.0	8974	0.79	0.3

Power spectrum of estimated forces at directions X, and the power spectrum of simulated force in harmonic components and random noise presence are showed in Fig. 9.

As one can observe in Tab. 5 and Fig. 9, in this application the Next was very robust in relation to harmonics and random noise added to input.

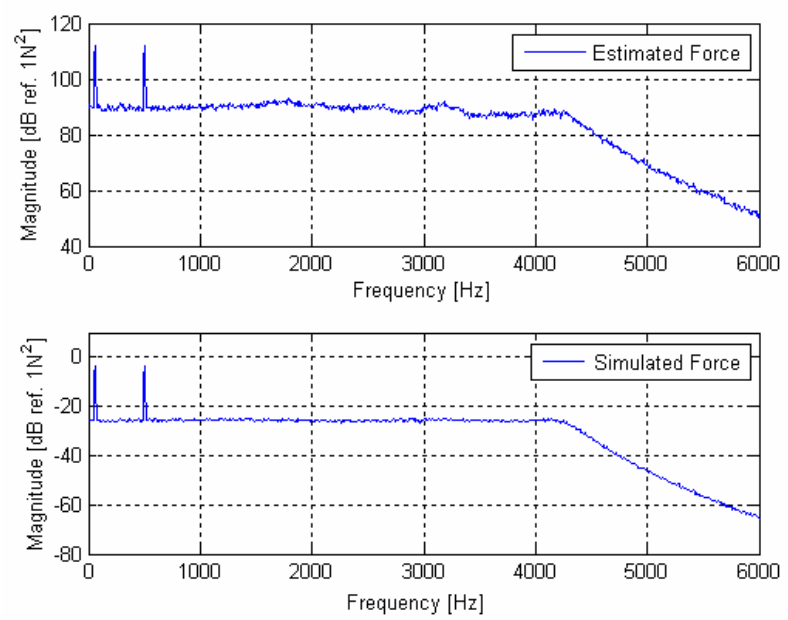

Figure 9. Power spectrum of estimated forces at directions X, and the power spectrum of simulated force in harmonic components and random noise presence.

5. CONCLUSIONS

The mainly conclusions of this work are:

- Next was shown as a very robust tool to identification of excitation forces by vibration monitoring at the studied model. So an unexplored field of researches in indirect triaxial forces monitoring to be applied in cutting machines.
- The developed methodology was show very insensitivity with relation to external randon and harmonics noise.
- A sensibility analysis to verify the best sensor location is important for the success of the methodology.

6. ACKNOWLEDGEMENTS

The authors would like to thank FAPEMIG (Research Support of Minas Gerais State Foundation), CNPq (National Counsel of Technological and Scientific Development) and FEMEC (School of Mechanical Engineering) at UFU (Federal University of Uberlândia) for their financial support.

7. REFERENCES

Alves, M. T. S., 2005, "Avaliação Numérica e Experimental dos Métodos ERA e ERA/OKID Para a Identificação de Sistemas Mecânicos". Dissertação de Mestrado, Universidade Federal de Uberlândia.

Brincker, R., Andersen, P., Muller, N., 2000, "An indicator for separation of structural and harmonic modes in output only modal testing", International Modal Analysis Conference (IMAC XVIII), San Antonio, TX, Society for Engineering Mechanics, Bethel, CT, 2000, pp. 1649–1654.

Hermans, L., Van Der Auweraer, H., 1999. "Modal Testing and Analysis of Structures under Operational Conditions: Industrial Applications". Mechanical Systems and Signal Processing 13(2), pp. 193-216

Juang, J. N., 1994, "Applied System Identification", Prentice Hall PTR, Englewood Cliffs, New Jersey, USA.

Mohanty, P., Rixen, D.J., 2003. "A Modified Ibrahim Time Domain Algorithm for Operational Modal Analysis Including Harmonic Excitation". Journal of Sound and Vibration 275 pp. 375–390

Nunes, O. A. J., 2006. "Identificação dos Parâmetros Modais Utilizando Apenas as Respostas da Estrutura-Identificação no Domínio do Tempo". Dissertação de Mestrado, Universidade Estadual Paulista – Unesp, Ilha Solteira- SP.

Silva, B. E. P., Pereira, J. A., Freitas, T. C., 2007, "Influência dos Componentes Harmônicos na Análise Modal Operacional de um Sistema Massa-Amortecedor-Mola de 5gl(S)", 7th Brazilian Conference on Dynamics, Control and Applications.

Zhang, L., Brincker, R. e Andersen, P., 2005, "An Overview of Operational Modal Analysis: Major Development and Issues".

7. RESPONSIBILITY NOTICE

The authors are the only responsible for the printed material included in this paper.